Ciprofloxacin-Protected Gold Nanoparticles

Renjis T. Tom,[†,‡] V. Suryanarayanan,[†,‡] P. Ganapati Reddy,[†] S. Baskaran,[†] and T. Pradeep*[,†,‡]

Department of Chemistry and Regional Sophisticated Instrumentation Centre, Indian Institute of Technology Madras, Chennai 600 036, India

Received October 4, 2003. In Final Form: November 24, 2003

The antibacterial drug ciprofloxacin (cfH) has been used to protect gold nanoparticles of two different mean diameters, 4 and 20 nm. The protection is complete with about 65 and 585 cfH molecules covering 4 and 15 nm particles, respectively. The nature of binding has been investigated by several analytical techniques. The nitrogen atom of the NH moiety of piperazine group binds on the gold surface, as revealed by voltammetric and spectroscopic studies. The cfH-adsorbed particles are stable in the dry state as well as at room temperature, and as a result, redispersion is possible. The rate of release of the drug molecule from the nanoparticles is more in the basic medium than in pure water, and the kinetics depend on the size of the particle; faster desorption is seen in smaller particles. The bound cfH is fluorescent, and this property could be used in biological investigations. This study shows that metal nanoparticles could be useful carriers for cfH and fluoroquinolone molecules. Most of the bound molecules could be released over an extended period of time.

Introduction

Availability of diverse nanoparticles with controlled properties has generated widespread interest in their use in biological systems. The fact that nanoparticles are comparable in size range to many common biomolecules makes them natural companions in hybrid systems. There are analytical techniques based on combining functionalities of biomolecules and organic molecules incorporated on nanoparticles. These have been used in areas such as biosensing,[1,2] bioimaging,[3] catalytic asymmetric reactions,[4] and targeted drug delivery.[5] Gold nanoparticle conjugation has been utilized for polynucleotide detection, in a way exploiting the alteration in optical properties resulting from the interparticle electronic interactions between adjacent nanoparticles.[6] In this context, we have reported the detection of a pesticide, endosulfan, in sub-ppm levels by gold nanopaticles.[7] Bioelectrocatalytic oxidation of glucose to gluconic acid with reconstitution of an apoflavoenzyme, apoglucose oxidase, on a 1.4 nm sized gold nanocrystal functionalized with cofactor flavin adenine dinucleotide has been reported.[8] Ion-selective biocompatible films of TiO_2 nanoshells were used for neurochemical monitoring.[9] Efficient optical[10] and electrochemical[11,12] sensing of biomolecules by gold nanoparticles is a popular area of research. Synthesis of nanoparticles using microorganisms is also well-known.[13] With selected biomolecules bound to metal nanocluster surfaces, new "hybrid" nanostructures can be obtained for applications such as drug delivery. Metal nanoclusters can be embedded in other biocompatible materials to modify material properties or to impart new functionality. In addition to this, one can make modifications of nanoclusters to better suit their integration with biological systems; for example, modifying their surface layers can enhance aqueous solubility, biocompatibility, and biorecognition.[14] The drug release must be controlled so that therapeutic molecules are delivered in desired patterns. Halas et al., using gold nanoshell−polymer nanocomposites,[5] reported a photothermally triggered drug delivery system. Previous work had focused on achieving specific drug release patterns by the use of electric and magnetic fields, ultrasound, light and enzymes, as well as using microsized pumps, valves, and channels.[15]

With improvements that are being made in the field of nanotechnology, the future of such devices in biomedical applications and drug delivery looks very promising. Interactions of nanoparticles with biologically active molecules have to be studied to understand the processes in detail. In this paper, we studied the functionalization of nanoparticle surfaces with cfH, investigated the interaction sites, and correlated the adsorption/desorption properties with structure. This is the first report in which a cfH molecule is used as the capping agent for gold nanoparticles. While there have been several literature reports on drug−nanoparticles interaction, only limited information is available on the nature of binding. We chose the cfH molecule to study the interaction because the system can be probed in detail with several instrumental

* To whom correspondence should be addressed. E-mail: pradeep@iitm.ac.in. Fax: 00-91-44-2257-0509 or 0545.

† Department of Chemistry.

‡ Regional Sophisticated Instrumentation Centre.

(1) Bruchez, M., Jr.; Moronne, M.; Gin, P.; Weiss, S.; Alivisatos, A. P. *Science* **1998**, *281*, 2013−2016.

(2) Lahav, M.; Shipway, A. N.; Willner, I. *J. Chem. Soc., Perkin Trans. 2* **1999**, 1925−1931.

(3) Djalali, R.; Chen, Y.; Matsui, H. *J. Am. Chem. Soc.* **2002**, *124*, 13660−13661.

(4) Li, H.; Luk, Y.-Y.; Mrkvsich, M. *Langmuir* **1999**, *15*, 4957−4959.

(5) West, J. L.; Halas, N. J. *Curr. Opin. Biotechnol.* **2000**, *11*, 215−217.

(6) Elghanian, R.; Strhoff, J. J.; Mucic, R. C.; Lestinger, R. L.; Mirkin, C. A. *Science* **1997**, *277*, 1078−1081.

(7) Nair, A. S.; Tom, R. T.; Pradeep, T. *J. Environ. Monit.* **2003**, *5*, 363−365.

(8) Xiao, Y.; Patolsky, F.; Katz, E.; Hanifeld, J. F.; Willner, I. *Science* **2003**, *299*, 1877−1880.

(9) Koktysh, D. S.; Liang, X.; Yun, B.-G.; Pastoriza-Santos, I.; Matts, R. L.; Giersig, M.; Serra-Rodriguez, C.; Liz-Marzan, L. M.; Kotov, N. A. *Adv. Funct. Mater.* **2002**, *12*, 255−265.

(10) Nath, N.; Chilkoti, A. *Anal. Chem.* **2002**, *74*, 504−509.

(11) Raj, C. R.; Okajima, T.; Ohsaka, T. *J. Electroanal. Chem.* **2003**, *593*, 127−33.

(12) Lahav, M.; Shipway, A. N.; Willner, I.; Neilsen, M. B.; Stoddart, J. F. *J. Electroanal. Chem.* **2000**, *482*, 217−221.

(13) Nair, B.; Pradeep, T. *Cryst. Growth Des.* **2002**, *2*, 293−298.

(14) Hussain, N.; Singh, B.; Sakthivel, T.; Florence, A. T. *Int. J. Pharm.* **2003**, *254*, 27−31.

(15) Langer, R. *Acc. Chem. Res.* **2000**, *33*, 94−101.

10.1021/la0358567 CCC: $27.50
Published on Web 01/24/2004

techniques, even when the concentration is small. Fluoroquinolones such as ciprofloxacin [1-cyclopropyl-6-fluoro-1,4-dihydro-4-oxo-7-piperazinylquinolone-3-carboxylic acid], clinofloxacin, levofloxacin, norfloxacin, and sparofloxacin are antibacterial agents that have gained wide acceptance for the treatment of a range of bacterial infections.[16] We are aware of the fact that application of such functionalized nanopaticles in living systems requires additional work. We undertook this research as part of our ongoing efforts on monolayer protected clusters[17] and core−shell nanoparticles.[18]

Experimental Section

$HAuCl_4 \cdot 3H_2O$, trisodium citrate, sodium bicarbonate, and 2-propanol were purchased from CDH chemicals. Potassium bromide (spectroscopic grade) was from Merck. Sodium borohydride was from Aldrich. cfH was prepared by our newly developed methodology as given below.[19] It was also purchased from Fluka.

Modified Procedure for the Preparation of cfH under Microwave Conditions. A mixture of 1-cyclopropyl-7-chloro-6-fluoro-4-oxo-1,4-dihydroquinoline-3-carboxylic acid (282 mg, 1.0 mmol) and piperazine (301 mg, 3.5 mmol) in DMSO (1.5 mL) was irradiated in an unmodified domestic microwave oven at power setting 2 for 20 min (2 × 10 min pulse). The reaction mixture was cooled to room temperature, triturated with 30% aqueous 2-propanol solution (3 mL), allowed to stand at 0 °C for 1 h, and then filtered. The solid was washed with water (2 mL) and dried under high vacuum to afford pure ciprofloxacin (280 mg, 84% yield, HPLC purity 99.84%) as an off white solid, mp 250−253 °C (dec).

^{1}H NMR (400 MHz, $CDCl_3$): δ 8.75 (s, 1H), 7.94 (d, J = 13.2 Hz, 1H), 7.45 (d, J = 7.4 Hz, 1H), 3.64−3.75 (m, 1H), 3.32−3.37 (m, 5H), 3.11 (t, J = 4.3 Hz, 4H), 1.38−1.48 (m, 2H), 1.22−1.25 (m, 2H).

HPLC conditions: column, Inertsil ODS-2, 25 cm, 4.6 mm, 5 μm (GL sciences); flow rate, 1.0 mL/min; temperature, 35 °C; mobile phase, 45% buffer solution (to a solution of 0.05 M sodium lauryl sulfate was added 0.1% triethylamine and the pH of the solution was adjusted to 3.0 using 0.1 M phosphoric acid) in acetonitrile; sample concentration, 0.1 mg/mL in acetonitrile.

All the solvents used in the synthesis were from local sources and were distilled prior to use. The chemicals were of the best purity available. The purity was not independently checked except for UV/vis absorption spectroscopy, wherever necessary. Triply distilled water was used throughout the work.

(i) Synthesis of Citrate-Capped Gold Nanoparticles of 3−4 nm[20] and 15−20 nm[21] Mean Diameter. An 18.5 mL volume of water and 0.5 mL of 10^{-2} M trisodium citrate were mixed well. To this was added 0.5 mL (1 mM) of chloroauric acid, and the mixture was stirred and then cooled in an ice bath. To the above mixture, 0.1 M of sodium borohydride (0.5 mL) was added slowly and stirred until the color turned to orange. The nanoparticles gave a characteristic absorption at 507 nm in the UV−visible spectrum. From the TEM measurements, the size of the nanoparticles was noted as 3−4 nm. For preparation of gold nanoparticles of 15−20 nm size, the same concentration of aqueous trisodium citrate and chloroauric acid mentioned in the previous procedure was taken and refluxed together until the color changed to wine red. In this case, the trisodium citrate itself acted as the reducing agent instead of sodium borohydride. The concentration of both the sols was 0.5 mM.

(ii) Synthesis of cfH-Coated Gold Nanoparticles. A 20 mL volume of citrate-capped gold nanoparticle solution (0.5 mM) was mixed with 5 mL of 2.5 mM cfH in 2-propanol and stirred effectively. The observed pH was 6.2. Stirring was continued for 8 h until the wine red color changed to blue and the pH was still acidic. The solution was centrifuged to obtain the precipitate of cfH-covered gold nanoparticles. The time-dependent UV−visible spectra were recorded after mixing cfH with nanoparticles at time intervals of 30 min (see Supporting Information). The blue colored solution was kept overnight without disturbing. The solution was centrifuged, and the precipitate was washed three times with 2-propanol and cold water to remove any unadsorbed cfH and unreacted borohydride/citrate. The washed precipitate can be dispersed easily in organic solvents such as DMSO, DMF, 2-propanol, and 1-butanol by sonication. The solutions were stable for several days.

The samples were characterized by UV−visible spectroscopy (Perkin-Elmer Lambda 25), transmission electron microscopy (TEM, 120 kV, Philips CM12), infrared spectroscopy (FTIR, Perkin-Elmer Spectrum One), FT-Raman spectroscopy (Bruker IFS66 infrared spectrometer, 1064 nm Nd:YAG laser), optical emission spectroscopy (F-4500 Hitachi Spectroflourometer), mass spectroscopy (MALDI-TOF MS, Kratos Analytical, Alpha Discovery with sinapinic acid (3,5-dimethoxy-4-hydroxycinnamic acid) as the matrix and 337 nm N_2 laser), and ^{19}F nuclear magnetic resonance spectroscopy (Bruker WM 400 spectrometer operating at 376.5 MHz; chemical shifts referenced with respect to trifluoroacetic acid in D_2O). Cyclic voltammetry (electrochemical analyzer, CH Instruments Model 600A) was performed using in a standard three-electrode cell comprising a Pt disk (area = 0.8 mm^2) as the working electrode, a platinum foil as the counter electrode, and Ag/AgCl as the reference electrode.

Desorption profiles were obtained as follows. A 20 mL volume of aqueous dispersion of cfH-protected gold was mixed with 20 mL of 20 mM sodium bicarbonate solution, and the mixture was divided into 5 mL fractions. Each fraction was centrifuged as a function of time. The absorbance of each solution was monitored at different times. One sample solution was used only once so that there was no change in the concentration of the solution. The intensity of absorption was plotted against time which gave the desorption profile of cfH.

Results and Discussion

Changes in the absorption spectroscopic characteristics of gold nanoparticles upon adsorption of cfH are depicted in Figure 1. The colloidal solution containing citrate-capped gold nanoparticles (Au@cit, 20 nm) has very intense and characteristic wine red color originating from the coherent electron motion, which gives rise to the surface plasmon absorption at 524 nm in the UV−visible spectrum (curve a). After addition of cfH, quenching of the characteristic absorption plasmon band is observed which follows a shift to the longer wavelength. This was also reflected in the change in color of bare Au@citrate nanoparticles from red to purple to bluish purple and finally to blue as a consequence of aggregation. The UV−visible spectra of cfH adsorbed gold nanoparticles were also recorded in different organic solvents such as dimethyl sulfoxide (DMSO), *N*,*N*-dimethylformamide (DMF), 1-butanol, and 2-propanol. Similarity in the spectral pattern in aqueous as well organic systems confirms the existence of colloidal aggregation in the organic phase as well (see the Supporting Information). The absorption in the 250−350 region show three distinct absorption bands at 271, 324, and 335 nm corresponding to the absorption of cfH molecule (curve c). The absorption maximum at 271 nm corresponds to the $\pi-\pi^*$ transition of the fluorobenzene moiety, and other two correspond to $n-\pi^*$ as well as $\pi-\pi^*$ transitions of the quinolone ring[22] (the structure of the molecule is shown in Chart 1). After adsorption, the peak

(16) Drakopoulos, A. I.; Ioannou, P. C. *Anal. Chim. Acta* **1997**, *354*, 197−204.
(17) Sandhyarani, N.; Pradeep, T. *Int. Rev. Phys. Chem.* **2003**, *22*, 221−262.
(18) Tom, R. T.; Nair, A. S.; Singh, N.; Aslam, M.; Nagendra, C. L.; Philip, R.; Vijayamohanan, K.; Pradeep, T. *Langmuir* **2003**, *19*, 3439−3445.
(19) Reddy, P. G.; Baskaran, S. *Tetrahedron Lett.* **2001**, *42*, 6775−6777.
(20) Obrae, S. O.; Rachael, E.; Hollowell, R. E.; Murphy, C. J. *Langmuir* **2002**, *18*, 10407−10410.
(21) Turkevich, J.; Stevenson, P. C.; Hillier, J. *Discuss. Farady Soc.* **1951**, *11*, 55−75.
(22) Zupancic, M.; Arcon, I.; Bukovec, P.; Kodre, A. *Croat. Chem. Acta* **2002**, *75*, 1−12.

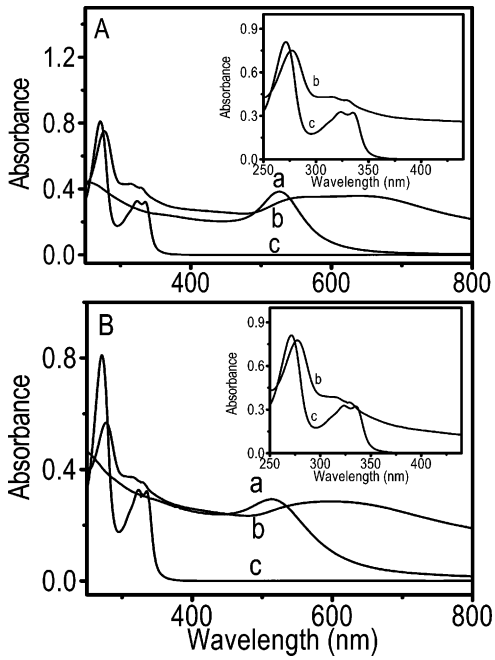

Figure 1. UV−visible spectra of gold nanoparticles upon adsorption of cfH (0.25 mM) taken in aqueous medium: (A) 15−20 nm particles; (B) 3−4 nm particles. Curves a−c correspond to pure nanoparticles, particles after stirring with cfH for 8 h, and pure cfH, respectively. The baseline shift in (b) of both (A) and (B) is due to aggregation. Insets in (A) and (B) show expanded views of the respective spectra in the 250−450 nm region. Curves b and c correspond to the same description as above.

Chart 1. Structure of Ciprofloxacin

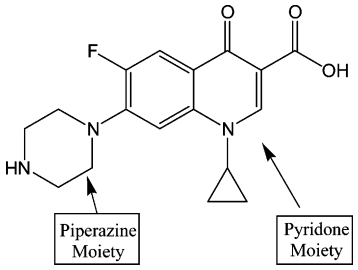

at 271 nm is shifted to 277 nm and the other absorption peaks of cfH molecules at 324 and 335 nm also get shifted to shorter wavelength (curve b; also see the inset of Figure 1A). The same behavior is also noted in the case of cfH added to Au@cit of 4 nm mean diameter (inset of Figure 1B). From the intensity of absorption of cfH molecules on the gold surface, the total number of adsorbed species and the corresponding surface area per cfH molecule can be calculated. The values are 65/cluster for 3−4 nm particles and 585 for 15−20 nm particles, suggesting a cross-sectional area of 3.09- and 4.84 nm^2/cfH molecule, respectively (see the Supporting Information). This rather large area/molecule and the difference in this value between the two particles is probably due to the partial coverage of the surface with citrate molecules as revealed by IR (see below).

In the TEM picture of adsorbed particles, aggregates of gold nanoparticles are clearly seen (Figure 2). Aggregation of these metal nanoparticles yields both a shift in the plasmon band energy and substantial increase in longer wavelength absorption as observed in the UV−visible spectrum.[23]

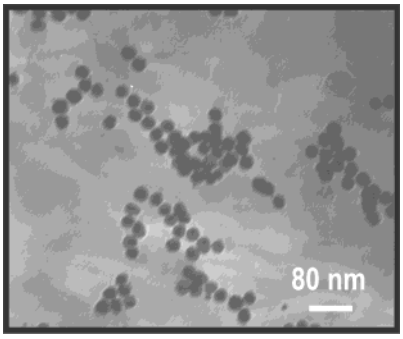

Figure 2. Transmission electron micrograph of cfH-covered gold nanoparticles of 20 nm average diameter. The sample was prepared from an aqueous solution.

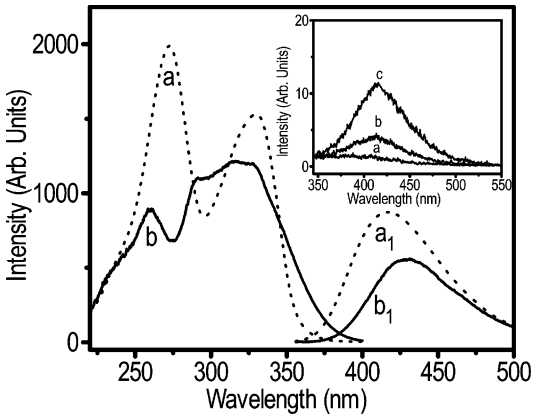

Figure 3. Excitation and emission spectra of (a, a_1) for free cfH (0.5 mM) and (b, b_1) for the adsorbed species on gold nanoparticles taken in aqueous medium. The inset shows emission spectra of centrifugates collected at different intervals of time (min) (a) 0, (b) 50, and (c) 100. The time refers to the period during which cfH was allowed to desorb from the nanoparticle surface in solution. Small differences between absorption and excitation spectra are attributed to instrumental parameters.

Fluorescence is an excellent probe for looking at the electronic characteristics of nanomaterials. In Figure 3, a and a_1 respectively show the excitation and emission spectra of free cfH. The curves b and b_1 correspond to the adsorbed species on gold. Free cfH has a broad emission peak around 415 nm, when excited at 323 nm.[24,25] The adsorbed species has an emission spectrum centered at 446 nm, with a decrease in fluorescence intensity from 222 (free) to 185 (adsorbed). The data are presented in Figure 3; the concentration of cfH was the same in both the cases, as determined by absorption spectroscopy. The observed red shift in the emission and quenching of the intensity can be attributed to the electronic interactions between the drug molecule and the gold nanoparticles. The red shift in emission peaks agrees with the shift in the absorption bands (Figure 1). The decreased fluorescence confirms that a large fraction of excited cfH molecules are quenched by the gold nanocore. The emission spectra of Figure 3 represent the excited states that survive the deactivation by the metal surface.[26] Fluorescence of cfH is due to planar fluoroquinolone moiety in the molecule. An interesting observation of these cfH-bound gold nanoparticles in water is the emergence of a major emission

(23) Kim, Y.; Johnson, R. C.; Hupp, J. T. *Nano Lett.* **2001**, *1*, 165−167.

(24) Navalon, A.; Ballesteros, O.; Blanc, R.; Vilchez, J. L. *Talanta* **2000**, *52*, 845−852.

(25) Lian, N.; Zhao, H.; Sun, C.; Chen, S.; Lu, Y.; Jin, L. *Microchem. J.* **2003**, *74*, 223−230.

(26) Ipe, B. I.; Thomas, K. G.; Barazzouk, S.; Hotchandani, S.; Kamat, P. V. *J. Phys. Chem.* **2002**, *106*, 18−21.

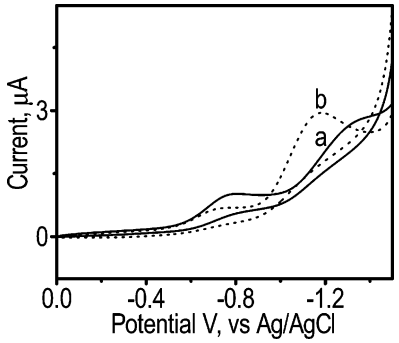

Figure 4. CV of (a) cfH (10^{-3} M) and (b) cfH adsorbed on Au nanoparticles (size 20 nm) taken on a Pt electrode in DMSO/(TBA)PF_6 at a sweep rate of 50 mV s^{-1}.

at 446 nm. Gold nanoparticles are nonfluorescent, and 0.5 mM cfH in water has strong emission at 415 nm. It is also observed that the absorption and emission characteristics have not changed with the size of the nanoparticles.

To check that the fluorescence intensity is only due to the adsorbed species, the solution used for the above measurement was centrifuged and the cfH-protected particles were removed. The fluorescence intensity of the centrifugate was measured without any dilution, and it was found that there was no appreciable amount of cfH desorbed during the span of the measurement. However, after time intervals of 50−100 min, the cfH adsorbed on gold begin to desorb which can be seen from the emission intensity. The inset shows percentage intensity of the species desorbed with respect to time. The data (Figure 3) suggest that bound cfH is fluorescent and desorption from the nanoparticle surface is insignificant on the experimental time scale. Note that bound and desorbed cfH have different absorption maxima.

The electrochemical properties of unadsorbed and adsorbed cfH molecules on nanogold surfaces were studied by cyclic voltammetry. Typical voltammograms of pure cfH molecule and adsorbed species (gold nanoparticles of 20 nm size) taken on Pt electrode in DMSO containing (TBA)PF_6 at a sweep rate of 50 mV s^{-1} are shown in Figure 4. cfH shows two cathodic reduction peaks at −0.81 and −1.25 V, which can be ascribed to the reduction of piperazinyl and pyridone moieties, respectively[27] (curve a of Figure 4). After adsorption, there is a considerable shift of peak potential of piperazinyl moiety to −0.79 V (the other peak also shifts from −1.25 to −1.23 V, curve b of Figure 4).

Further, a significant difference is noted in the CV obtained with different sweep rates of free cfH (Figure 5A) and adsorbed species (Figure 5B) where curves a−c correspond to sweep rates of 20, 50, 100 mV s^{-1}, respectively. The cathodic current of pyridone moiety of adsorbed cfH species increases considerably whereas the piperazinyl moiety does not show a corresponding increase. Plots of peak current vs square root of sweep rate (sweep rates other than 20, 50, and 100 mV s^{-1} are not shown in the CVs of Figure 5) during cathodic scanning (at −0.79 and −1.23 V for adsorbed and −0.81 and −1.25 V for unadsorbed) clearly show the difference between the adsorbed and unadsorbed species (inset in Figure 5A,B). From the above results, it is noted that piperazinyl ring is modified by the adsorption on gold nanoparticles, possibly through nitrogen whereas pyridone moiety is unaffected (Chart 2; see also below). The voltammetric

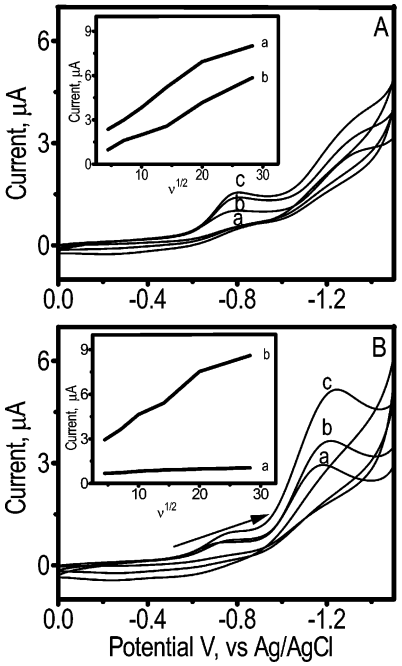

Figure 5. CV of (A) cfH (10^{-3} M) and (B) cfH adsorbed on Au nanoparticles taken on a Pt electrode in DMSO/(TBA)PF_6 at different sweep rates (a, 20, b, 50, and c, 100 mV s^{-1}) Insets a and b show the plots of peak current vs sweep rate obtained at −0.79 and −1.23 V for unadsorbed species (A) and 0.81 and −1.25 V for adsorbed species (B), respectively.

Chart 2. cfH−Au Nanoassembly

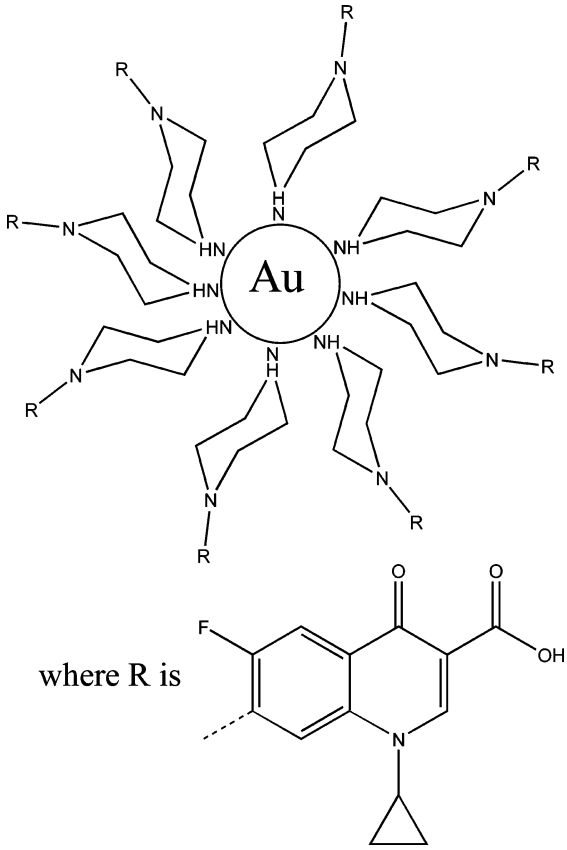

characteristics of cfH adsorbed on both 4 nm as well as 20 nm sized gold nanoparticles were found to be very similar.

The IR spectra of free cfH and the adsorbed one are shown in Figure 6. Absorption bands at 1725 and 1632 cm^{-1} are due to symmetric stretching of carbonyl group

(27) Saha, D. K.; Padhye, S.; Anson, C. E.; Powell, A. K. *Inorg. Chem. Commun.* **2002**, *5*, 1022−1027.

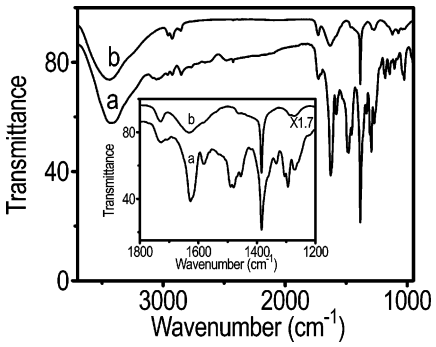

Figure 6. Infrared spectra of (a) free cfH and (b) cfH adsorbed on gold nanopartcles. The inset shows the expansion of the region from 1200 to 1800 cm^{-1}. Spectrum b in the inset has been shifted vertically to show the features clearly.

ν(C═O) of carboxylic acid and pyridone moieties, respectively.[28,29] The absorption band at 1286 cm^{-1} is due to the C−N stretching[28] (inset of Figure 6). The above-mentioned bands are shown by both absorbed and free cfH, confirming the presence of cfH moiety on the nanoparticle surface. The band at 3410 cm^{-1} is shifted to 3442 cm^{-1} and slightly broadened in the case of the adsorbed species. This band at 3410 cm^{-1} is due to the O−H stretching of the carboxylic acid moiety, and the shoulder at 3300 cm^{-1} is due to N−H stretching of the imino moiety of the piperazinyl group. The broad O−H stretching band is due to traces of water in the nanoparticle sample. The weak bands around 2900 cm^{-1} in the adsorbed species (b) are due to traces of citrate impurity in the sample.

Absorption bands in free cfH (a) around 1579 cm^{-1} and 1381 cm^{-1} are due to asymmetric ν_{as}(O−C−O) and symmetric ν_s(O−C−O) stretching of the carboxylic acid group, respectively (inset of Figure 6).[30] The band at 1381 cm^{-1} is shown by both adsorbed (b) and free cfH (a). The band at 1579 cm^{-1} is partially obscured by the broadened 1632 cm^{-1} band in the case of adsorbed cfH (b). From the above data it can be inferred that neither the keto group nor the carboxyl group directly binds to the gold surface, as would be expected chemically. Thus, only nitrogen atoms are likely to be involved in binding on the gold surface. The nitrogen atom of the quinolone ring and the one ortho to fluorine are less electron rich due delocalization of electrons to electron deficient fluoroquinolone ring. The cyclopropyl and piperazinyl groups sterically hinder them also. Thus, the only possibility is the involvement of the imino moiety of the piperazinyl group. However, the infrared spectrum is not definitive about it as the band profile is unclear due to the intense OH stretching.

In the FT-Raman (not shown) spectrum of the cfH-coated particles, bands at 1595 and 1389 cm^{-1} respectively due to asymmetric ν_{as}(O−C−O) and symmetric ν_s(O−C−O) stretching of carboxylic acid group are seen. A band at 1623 cm^{-1} due to symmetric stretching of the carbonyl group ν(C═O) of the pyridone moiety[30] is also seen. Both bound and free cfH show these features in the Raman spectrum.

A ^{19}F NMR study of cfH loaded poly(ethylbutylcyanoacrylate) (PEBCA) nanoparticles was reported by Page-Clisson et al.[31] The ^{1}H-coupled ^{19}F NMR spectrum clearly distinguishes the free cfH molecule and the adsorbed species at different chemical shift values (Figure 7). The chemical shifts of a doublet of doublet are −39.30 and −39.65 ppm for the free and adsorbed species, respectively. The coupling constant values are 7.5 and 13 Hz for the four-bond coupling and three-bond coupling,[32] respectively. The shift of the molecule bound on the cluster surface gets downfielded to 0.35 ppm. But both the bound and unbound cfH show the same splitting characteristics irrespective of the slight change in the chemical shift. The unbound cfH is the hydrochloride salt while the bound cfH is in the neutral form. The hydrochloride salt had to be used, as the neutral molecule is only sparingly soluble in water. As the chemical shift between the two forms is small, it can be concluded that the electronic environment of the fluoroquinolone ring system is essentially the same in both the cases.

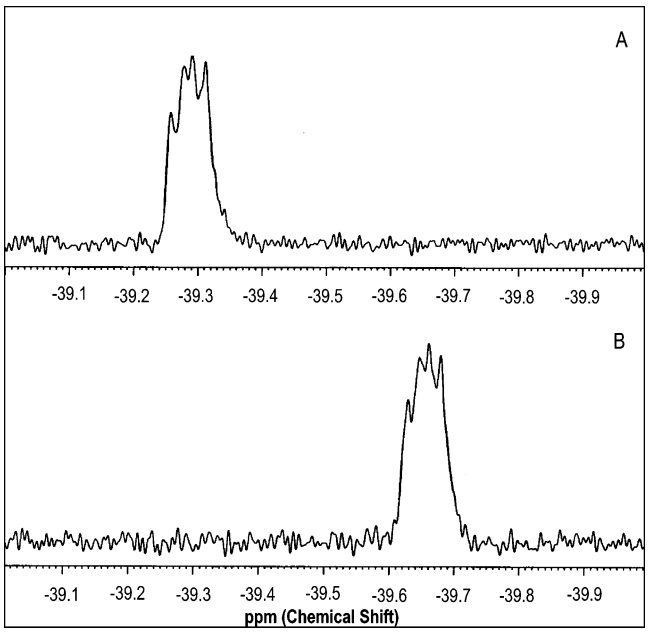

Figure 7. 376.5 MHz ^{1}H-coupled ^{19}F NMR spectra of (A) pure cfH hydrochloride and (B) cfH adsorbed on gold nanoparticles.

The presence of an integral cfH moiety on the gold nanoclusters was confirmed by the presence of the CfH_2^+ ion peak at *m/z* 332 in the MALDI spectrum. Both pure cfH and cfH-bound gold nanoparticles showed peaks at *m/z* 332, which is due to the protonated cfH molecule.[22,31] Thus, the compound retains its identity during adsorption on the cluster surface and can be desorbed in the integral form.

Base-catalyzed desorption[31] of cfH from gold nanoparticles was also carried out using the bicarbonate ion. A solution (20 mL) of cfH-capped gold nanoparticles (after washing with water and 1-propanol) was treated with a 20 mL aqueous sodium bicarbonate solution (20 mM), and the mixture was divided into 5 mL fractions. After each 100 min period, one solution was centrifuged. The centrifugate was analyzed by UV−visible spectroscopy, and the percentage of cfH molecules released was calculated. This was plotted against the time interval at which the analyte was withdrawn (Figure 8). From this plot, it is observed that gold nanoparticles of smaller size (4 nm; plot a) release cfH molecules faster than the large size species (20 nm, plot b). The release of cfH from the

(28) Wu, G.; Wang, G.; Fu, X.; Zhu, L. *Molecules* **2003**, *8*, 287−296.
(29) Zupancic, M.; Turel, I.; Bukovec, P.; White, A. J. P.; Williams, D. J. *Croat. Chem. Acta* **2001**, *74*, 61−74.
(30) Turel, I.; Bukovec, P.; Quiros, M. *Int. J. Pharm.* **1997**, *152*, 59−65.
(31) Page-Clisson, M. E.; Pinto-Alphandray, H.; Ourevitch, M.; Andremont, A.; Couvreur, P. *J. Controlled Release* **1998**, *56*, 23−32.
(32) Freeny, J.; McCormick, J. E.; Bauer, C. J.; Birdsall, B.; Moody, C. M.; Starkmann, B. A.; Young, D. W.; Francis, P.; Havlin, R. H.; Arnold, W. D.; Oldfield, E. *J. Am. Chem. Soc.* **1996**, *118*, 8700−8706.

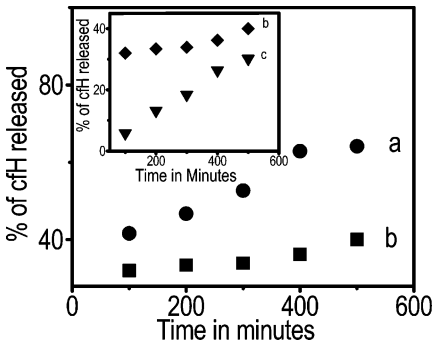

Figure 8. Time-dependent release of cfH molecules in the presence of 10 mM sodium bicarbonate solution (pH at 7.63) from gold nanoparticle surface. (Traces a and b represent the nanoparticles of sizes, 4 and 20 nm, respectively.) The release of cfH in neutral water for 20 nm sized gold clusters is compared in the inset. Traces b and c represent bicarbonate and water media, respectively.

nanoparticle surface was also compared in the neutral medium (in water) for 20 nm sized gold particles (inset of Figure 8). Trace b represents the bicarbonate medium, and c corresponds to the water medium. The release of cfH molecules is rapid in bicarbonate medium when compared to water medium. The exact mechanism of the release of cfH molecule is unknown.

Conclusion

Adsorption of cfH molecule on gold nanoparticle surface was studied using different analytical techniques. The nitrogen atom of the NH moiety of piperazine group can bind strongly to Au nanoparticles as confirmed by voltammetric and spectroscopic studies. The adsorbed species are stable in the dry state, and the material can be redispersed. The rate of release of the drug molecule from the nanoparticles is more in the bicarbonate medium than in water, which also depends on the size of the particle. This study shows that nanoparticles could be useful carriers for cfH molecule. Further studies will be oriented toward the optimization of the complete release of the molecule in a controlled fashion. Fluorescence of the adsorbed molecule suggests possible applications.

Acknowledgment. The nanoparticles research program of T.P. is funded by the Ministry of Information Technology and ISRO-IITM Cell. Equipment support is provided by the Department of Science and Technology through the Nanoscience Initiative. R.T.T. thanks the Council of Scientific and Industrial Research (CSIR) for a research fellowship. V.S. thanks the CSIR for a research associateship. Dr. R. V. Omkumar of Rajiv Gandhi Cenre for Biotechnology, Trivandrum, India, is thanked for MALDI studies.

Supporting Information Available: Time-dependent UV−visible spectra obtained after mixing cfH with gold nanoparticles in water medium, calculation of the surface coverage of the nanoparticles, and the UV−visible spectra of cfH-capped gold nanoparticles taken in different organic solvents. This material is available free of charge via the Internet at http://pubs.acs.org.

LA0358567